Proceedings of the 11th World Congress in Mechanism and Machine Science
August 18~21, 2003, Tianjin, China
China Machinery Press, edited by Tian Huang

Studies on a Stewart Platform based Force – Torque Sensor in a Near-Singular Configuration

R. Ranganath
Spacecraft Mechanisms Group, ISRO Satellite Centre, Bangalore – 560017, India.
e-mail: rrrr@isac.ernet.in

P. S. Nair
Structures Group, ISRO Satellite Centre, Bangalore – 560017, India.
email: psnair@isac.ernet.in

T. S. Mruthyunjaya, A. Ghosal
Dept. of Mechanical Engineering, Indian Institute of Science, Bangalore –560012.
email: tsmjaya@mecheng.iisc.ernet.in, asitava@mecheng.iisc.ernet.in

Abstract: For a mechanism at a near-singular configuration, a small applied force-torque in certain specific directions, can give rise to large forces in the links of the mechanism. This concept is used to design a near-singular flexure jointed Stewart Platform based force - torque sensor sensitive to forces and moments in certain desired directions. Detailed parametric studies and computer simulation of the resulting leg forces in the Stewart Platform due to externally applied forces and moments have been conducted. The suitability of the chosen configuration for magnification in leg forces for force-torque application in specific directions is experimentally verified on a prototype hardware.

Keywords: Stewart Platform, Sensor, Singular Configuration

1 Introduction

The Stewart Platform was originally proposed for a flight simulator by Stewart[17]. Several researchers have also proposed the use of a Stewart Platform as a six component force-torque sensor (see, for example, Gaillet and Reboulet[5], Rees[14], Kerr[9], Nguyen et al[11]., Romiti and Sorli[15], Sorli and Zhmud[16], Hongrui[8] et al., Dasgupta et al[3], and Dwarakanath et al[4].,). Typically, the force in the leg is measured in the form of strain and a strain sensing element such as strain gage is used. Several researchers (for example, Champagne[2] et al.,), describe the design, fabrication, testing and operation of a flexure jointed six axis force and torque dynamometer near an isotropic configuration, where the sensitivity to the externally applied load is approximately same in all directions. Our goal is very different. We aim to design a Stewart Platform based force-torque sensor at a near-singular configuration, wherein the sensitivity will be high in certain predetermined directions of applied external force/torque. In these directions, due to the near-singular configuration of the Stewart Platform there will be significant magnification of forces in the legs and very small external forces/moments can be sensed easily. In other directions, the sensitivity will be that of a normal load sensor determined by the sensitivity of the sensing element. The singularities of serial and parallel manipulators have been extensively studied (see, for example, Gosselin and Angeles[7], Merlet[10], Ghosal and Ravani[6] and Basu and Ghosal[1] and the references therein.)

In this paper, the concept of force magnification is applied to a spatial spherical jointed Stewart Platform based force-torque sensor in a near-singular configuration and using the equation of statics, the magnification in the leg forces is shown clearly. Using FEM analysis, this concept is shown to be applicable for flexure jointed Stewart Platform sensor, as the flexure joints eliminate the inaccuracies associated with friction and backlash of normal joints. The concept of force magnification is validated by the development and testing of a prototype hardware of the flexure jointed Stewart Platform sensor in a near-singular configuration.

2 Statics of Stewart Platform Sensor

The Stewart Platform, as shown in figure 1, consists of six extensible legs (with prismatic joints in each leg) connected to the (moving) platform and (fixed) base with spherical(S) joints. The base and platform coordinate systems are taken to be parallel and aligned with each other. q_1, q_2 and q_3 are the angles of rotation of the platform about the platform coordinate axes, Xp, Yp and Zp respectively. In a general configuration, the Stewart Platform has six active degrees-of-freedom and by actuating the six prismatic joints, one can achieve arbitrary position and orientation of the moving platform. If an external force-moment is applied at the platform, we can obtain the axial forces in the legs required to keep the Stewart Platform in equilibrium. This forms the topic of the statics of the Stewart Platform and is well known (see, for example, Dasgupta et al[3] .,)The external force, **F** and the external moment, **M** act on the center of the platform at an angle a with the horizontal plane of the platform (and hence the base) and an angle b, which is the angle made by the projection of the **[F, M]** vector on the horizontal plane of the platform with platform X axis. **[F, M]** can be related to the leg forces **f** by

$$\mathbf{W} = [\mathbf{H}]\ [\mathbf{f}] \qquad (1)$$

where **W = [F , M]¢.** The matrix **[H]** is called the force transformation matrix which maps the leg forces to the applied wrench W. If det**[H]**=0, i.e., when the matrix **[H]** is singular, some component(s) of the externally applied **F** and **M** cannot be supported by the structure and it gains one or more degrees of freedom instantaneously. The eigenvectors corresponding to the zero eigenvalues of **[H]** when mapped to **F** and **M** give the singular directions, and the Stewart Platform cannot withstand any force/moment applied along the singular directions. If the Stewart Platform is in a *near-singular* configuration, then a small force/moment along the singular direction will lead to large axial force in one or more of the legs, and we will get large magnification.

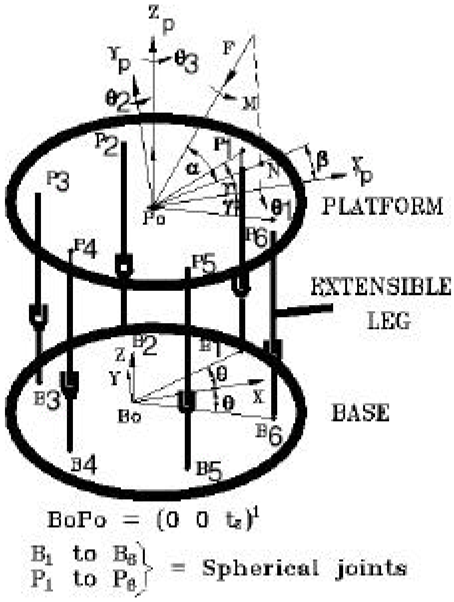

Figure 1: A 6 - 6 Stewart Platform

To arrive at a near-singular configuration, we perturb the symmetry of the connection points in the base and the platform. The half angles, g (gamma) and q (theta), between the leg connection points in the platform and base with Xp and X respectively, are initially 30°. Keeping θ as 30°, we change platform half angle around the nominal value of 30° from 25° to 35°. Figure 2 shows the variation of condition number as a function of g . It can be noted that at g =30°, the condition number of **[H]** is ∞ and falls off from ∞ on both sides of 30°. At g =33°, the condition number is approximately 1910 which is fairly large and we can expect significant magnification in the leg forces for external forces/moment applied along the singular directions F_x, F_y and M_z. We get more magnification in the leg forces if γ is chosen nearer to 30°, but the variation in the condition number is also larger if γ is nearer to 30°. The figure 3 shows the variation in the leg forces for g varying between 31° and 35°. It is observed that the slopes of the curves are small and for a small change in γ about 33°, the change in the slopes is not significant. For the above reasons, we choose γ =33° as the near-singular configuration. The nominal geometry of the Stewart Platform sensor with γ =33° is given in Table 1. It is to be noted that the Z coordinate of the base and platform are 0 and 100 mm respectively.

We next perturb the orientation of the platform by rotating about the platform Z axis. The figure 4 shows the plot of leg forces due to perturbation of θ_3 (theta3) around the nominal value of 0° respectively. We can observe that for a variation of ± 10° about nominal, the leg forces change significantly as seen in figure 4. Further, the platform was perturbed about θ_1 and θ_2 respectively, one at a time, for a range of ± 5° about the nominal position. It was observed that the leg forces do not change significantly for small changes in θ_1 and θ_2, which could occur due to external forces and moments acting on the Figure 2: Plot of condition no. of [H] with gamma platform and also due to tolerances in fabrication of the sensor.

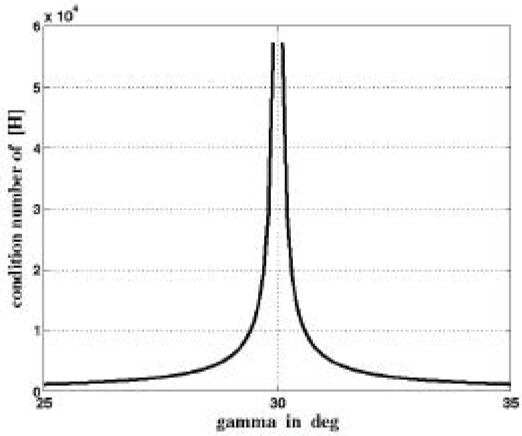

Figure 2: Plot of condition number with gamma

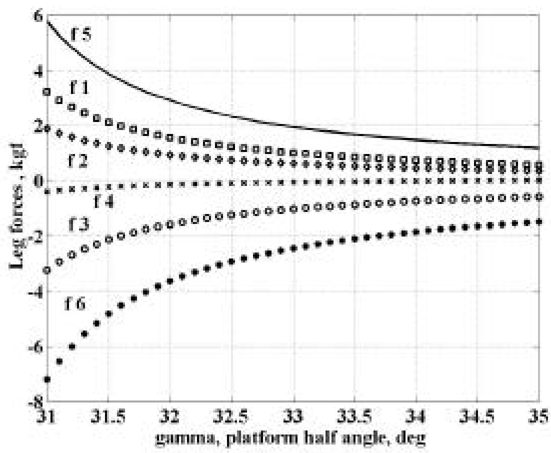

Figure 3: Plot of leg forces with gamma

Table 1: Nominal geometry of 6 - 6 Stewart Platform with g = 33 deg.

Base coordinates			Platform coordinates		
	x (mm)	y(mm)		x(mm)	y(mm)
B1	43.3	25.0	P1	41.93	27.23
B2	0	50	P2	2.62	49.93
B3	-43.3	25	P3	-44.55	22.70
B4	-43.3	-25	P4	-44.55	-22.70
B5	0	-50	P5	2.62	-49.93
B6	43.3	-25	P6	41.93	-27.23

The figure 5 shows the variation of leg forces as a function of the translation of the platform, tx, along the platform X direction around its nominal value. We observe that, the variation in the leg forces is about 10 %. A similar variation in leg forces was observed for the translation of the platform along the Y direction of the sensor. The leg forces do not show much change for the translation of the platform along the Z axis of the platform. The perturbation was also carried out for the variation of the platform radius **r** and base radius **R** about the nominal value of 50 mm and it was found that the variations in leg forces were not significant. The conclusion is that the sensitive directions of the sensor are along the X and Y directions for external force application and about Z direction for moment application. Hence, we conclude that the platform must be designed to be reasonably stiff along the platform X and Y directions and rotations about Z direction so as not to affect the desired magnification significantly.

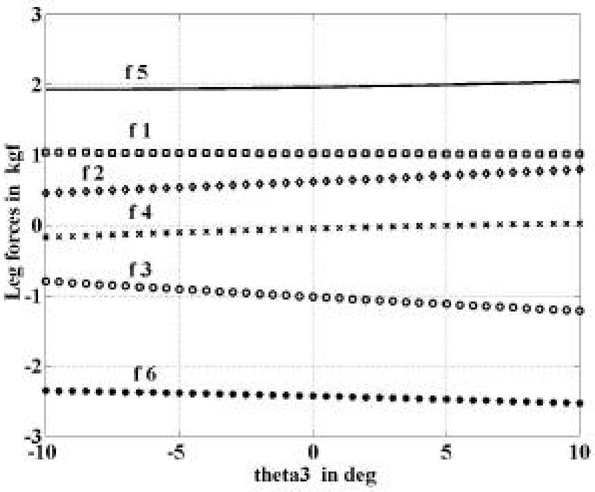

Figure 4: Plot leg forces with theta3

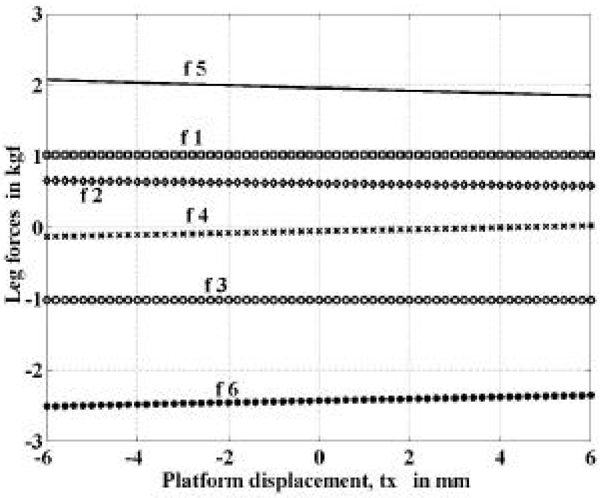

Figure 5: Plot of leg forces with tx

The sensitive directions of the sensor considered were verified independently by developing an algorithm, which also gave the sensitive directions for the sensor when the legs were connected in different sequences between the base and the platform.

3. Spherical joint replaced by flexure joint

The above analysis of the magnification of forces in the links was based on frictionless hinges which causes the forces in the links AC and BC to be purely axial (tension or compression). In practice, any hinge has friction, backlash and other non-linearities which will modify the axial forces in unpredictable ways. To avoid these problems, flexural hinges have been used in many applications such as gyroscopes, accelerometers and missile control nozzles.

A simple two axes flexure hinge with intersecting axes is formed by necking down a round bar as shown in figure 2. From the expressions for angular compliance (see Paros and Weisbord[10]), one can observe that the angular compliances become large as the thickness **t** of the necked region reduces, and approximates a two axes hinge for small **t**. At the same time, the longitudinal compliance also increases with decrease in **t**. However, the longitudinal compliance is proportional to $\mathbf{t}^{-3/2}$ whereas the angular compliance is proportional to $\mathbf{t}^{-7/2}$. Hence, a careful choice of **t** is required to obtain acceptable angular compliance and, at the same time, an acceptable stiffness in the longitudinal direction.

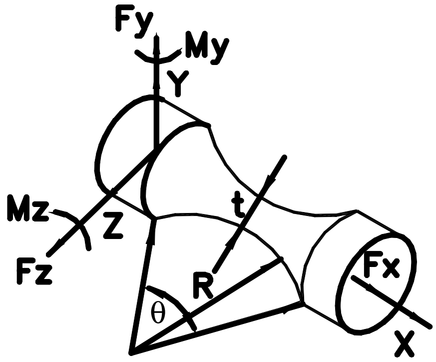

Figure 6: Flexure Hinge

4. FEM Analysis of the Stewart Platform Sensor

In the previous numerical results, it is assumed that the joints of the Stewart Platform are spherical (ball joints). We now replace the spherical joints by flexural hinges. The nominal 6-6 configuration has been modeled in a finite element analysis software package, NISA[16]. The ring sensor, 2 mm in thickness along the radius and 5 mm in width, is introduced in each of the legs and is modeled with plate elements. The leg and the flexure hinges are modeled with 3D beam elements. The diameter of the leg is 6 mm. The platform has been modeled with plate elements of thickness 5 mm. The material chosen for the legs is Titanium alloy (Ti-6Al-4V) for high strength, with a Young's modulus of 11200 kgf/mm^2 and a Poisson's ratio of 0.3. The material chosen for the base and the platform is an Aluminum alloy (for lower self weight) with an Young's modulus of 7070 kgf/mm^2 and a Poisson's ratio of 0.3. The boundary conditions to the base points at which the sensor is fixed to the ground are assigned zero displacement ($U_x=U_y=U_z=0$) and zero rotation ($R_x=R_y=R_z=0$) boundary conditions. The top and bottom end of the legs are node merged to the platform and base respectively. The FEM model has totally around 25400 degrees of freedom. The external loads, applied at the centre of the platform, are $F_x=F_y=F_z=0.1$ kgf and $M_x=M_y=M_z=5$ kgf-mm. The diameter of the flexure hinge in the legs is varied and the resulting FEM model is analyzed and the leg forces in the beam element of the leg above the ring sensor in the leg are presented in the Table 2. It is seen that as the kink diameter decreases, the axial forces in the legs approach the value obtained from statics with spherical joints. Further, for the case of kink of 0.5 mm square section, all the forces and moments acting on the node in the beam element near the ring sensor in the legs were calculated. It was observed that the transverse forces and moments become small and the axial forces dominate. Though the axial forces in the case of the kink diameter of 0.25 mm are closer to numerical results obtained with spherical joints, from manufacturing considerations , the kink of 0.5 mm square is chosen. A local overload protection in bi-axial bending is provided for the flexure. The length of the flexure joint is 1 mm. It is to be noted that [H] as defined in equation 1, is with reference to base coordinate system. Hence, a force F× applied at the platform center is equal to a force F× at the base and a moment of (F×*tz) about the Y axis at the base, as shown in figure 1. Likewise, a force Fy applied at the platform center is equal to a force Fy at the base and a moment of (-Fy*tz) about the X axis at the base, as shown in figure 1.This was considered for obtaining the results in column 2 of table 2 and also for the leg forces in figure 3.

For the externally applied loading of F_x=F_y=F_z=0.1 kgf, M_x=M_y=M_z=5 kgf-mm, the maximum deformation is obtained to be 0.5 mm for the top platform and the maximum stress is seen to be about 30 kgf/mm^2 at the flexible hinges. These are well within the allowable values of deflection of the platform and the maximum allowable stresses in the material. The maximum stress seen is in the ring elements which is 4 kgf/mm^2 and is far below the yield stress of around 90 kgf/mm ^{2}. The natural frequencies were evaluated from the FEM model of the sensor. The first, second and the third natural frequencies were found to be 22.38, 22.71 and 46.02 Hz respectively. The corresponding mode shapes were found to be in the XZ, YZ and XY planes respectively, the first two in bending mode and the third in torsion mode. This indicates that the sensor is reasonably stiff about the sensitive axes of the sensor.

5. Hardware realization and experimentation

The orthographic views of the Stewart Platform sensor are shown in the figure 7. A prototype of the Stewart Platform sensor, as designed above, was fabricated.

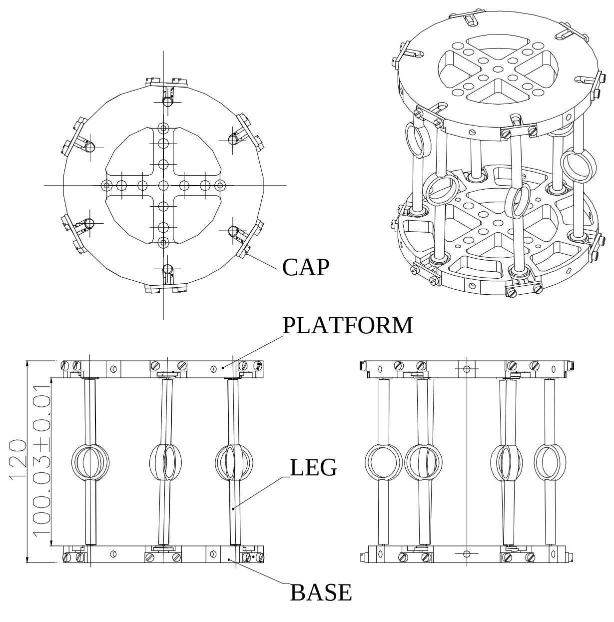

Figure 7: Orthographic views of the sensor

In this prototype, each leg with the flexible hinges and ring sensing element, is machined from a single piece of Titanium alloy. These were then assembled with the platform and base. Although it is well known that the entire sensor should be monolithic to avoid hysteresis effects, in this prototype the legs are assembled to the platform and base with screws torqued sufficiently to avoid slippages. This is because our aim is to demonstrate sensitivity to external loads in certain directions and hence the externally applied loads are chosen to be low in the sensitive directions. An additional goal is to use the *same legs* for other near-singular Stewart Platform based sensors and demonstrate sensitivity to external loads applied along different directions at a later date.

Figure 8 shows the prototype hardware being calibrated by applying the moments about the Z axis of the sensor. The maximum applied moment is 5.15 Kgf-mm. Similar moments were also applied about X and Y axes of the sensor, one at a time. The leg forces evaluated from the strain gauge readings are shown in the figure 9. It is seen clearly that the leg forces show considerable magnification for moments acting about Z direction in comparison to moments acting about X and Y directions respectively.

Figure 10 shows the results of the calibration of the sensor by the application of the force along X, Y and Z axes respectively, one axis at a time. The sensor is calibrated by gradually applying loads by means of standard calibrated weights upto a maximum of 0.103 Kgf. The microstrain readings in the legs are converted to

Table 2: Axial forces in the legs

Sl. no	Sph. Joint Results (Kgf)	Flexure joints (Leg forces in Kgf)			
		Dia in mm			Sq.in mm
		1	0.5	0.25	0.5
1	1.0175	0.340	0.873	0.980	0.810
2	0.6178	0.089	0.491	0.606	0.428
3	-1.0148	-0.120	-0.791	-0.967	-0.690
4	-0.0502	-0.072	-0.091	-0.079	-0.099
5	1.9588	0.659	1.701	1.930	1.571
6	-2.4290	-0.796	-2.084	-2.370	-1.919

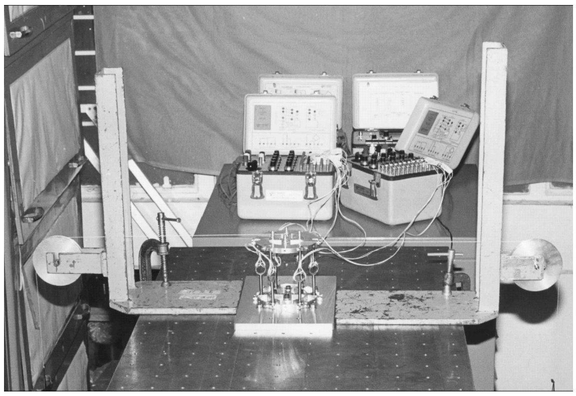

Figure 8 Test setup for Mz calibration

leg forces by the calibration factor of each of the individual legs. For loading along the X direction, a magnification of nearly 5 is seen in the legs 1,3,4 and 6. In legs 2 and 5, the magnification is nearly 10. For loading along Y direction, a magnification of nearly 10 is seen in the legs 1,3,4 and 6. It is also seen that no magnification is observed for loading in Z direction. The figures 9 and 10 clearly demonstrate the magnification of the leg forces in specific directions of force-moment application in a near-singular configuration

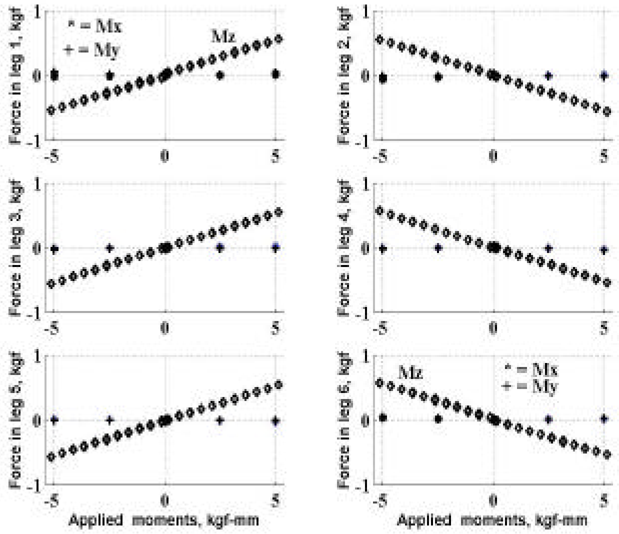

Figure 9 Leg forces for moment loads

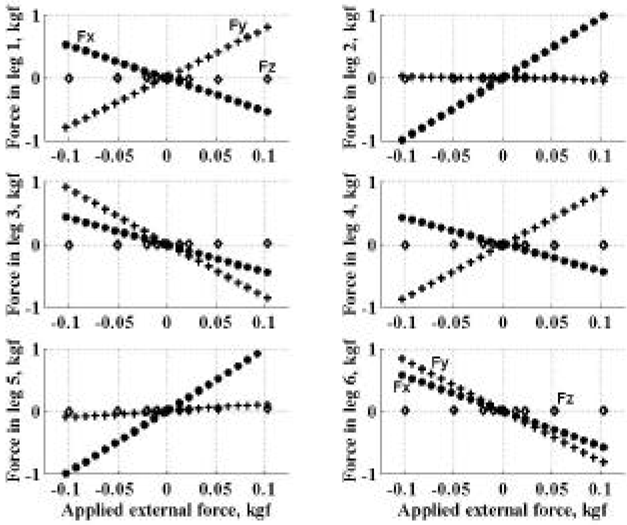

Figure 10 Leg forces for lateral loads

6. Conclusions

This paper deals with the analysis and design of a Stewart Platform based force/torque sensor in a *near- singular* configuration. The key idea that the external forces and moments applied on the platform in a near- singular configuration produces large forces in the legs of the sensor, is used to configure the force-torque sensor. Detailed numerical simulations show that it is indeed possible to obtain magnification in leg forces for application of forces and moments in specific directions at a near-singular configuration for a Stewart Platform, thereby making it possible to measure small forces acting on the platform in specific directions more accurately. Perturbation analysis of the geometric parameters of the sensor show that the leg forces do not vary significantly for small displacements of the platform, which could be due to external loading. The spherical joints in the sensor are replaced by flexure joints to eliminate the inaccuracies which could result from friction and backlash of normal joints. It is shown by FEM analysis, that the magnification in leg forces indeed exists even for flexure jointed Stewart Platform sensor. The concept of magnification in leg forces is validated by the development and testing of a flexure jointed prototype hardware.

Acknowledgements

The authors wish to thank Nageswara Rao, M. and Sridhara, C. D., of Spacecraft Mechanisms Group, ISRO Satellite Centre, Bangalore, for their encouragement in this work. Thanks are due to Dr. Badari Narayana, K., Structures Group , ISRO Satellite Centre, Bangalore, for helpful tips in using NISA package.

References

1. Basu, D. and Ghosal, A., Singularity analysis of platform-type multi-loop spatial mechanisms, *Mechanism and Machine Theory*, 32(3): 375-389, 1997.
2. Champagne, P. J., Cordova, S. A., Jacoby, M. S. and Lorell, K. R., Development of a precision six axis laboratory dynamometer, *NASA-CP-3147, 26th Aerospace Mechanisms Symposium*, 331-348, 1992.
3. Dasgupta, B., Reddy, S., and Mruthyunjaya, T. S., Synthesis of a force-torque sensor based on the Stewart Platform mechanism, In: *Proc. National Convention of Industrial Problems in Machines and Mechanisms (IPROMM'94)*, Bangalore, India, 14-23, 1994.
4. Dwarakanath, T. A., Dasgupta, B., and Mruthyunjaya, T. S., Design and development of a Stewart Platform based force-torque sensor, *Mechatronics*, 11:793-809, 2001.
5. Gaillet, A. and Reboulet, C., A isostatic six component force and torque sensor, In: *Proc. of the 13 Int. Conf. on Industrial Robotics*, 18.102-18.111, 1983.
6. Ghosal, A., and Ravani, B., A differential geometric analysis of singularities of point trajectories of serial and parallel manipulators, *Trans. of ASME, Journal of Mechanical Design*, 123: 80-89, 2001.
7. Gosselin, C. and Angeles, J., Singularity analysis of closed loop kinematic chains, *IEEE Trans. of Robotics and Automation*, 6(3): 281-290, 1990.
8. Hongrui, W., Feng, G., and Huang Zhen, H., Design of six axis force/torque sensor based on Stewart Platform related to isotropy, *Chinese Journal of Mechanical Engineering*, 3: 1998.
9. Kerr, D. R., Analysis, properties and design of Stewart platform transducer, *Trans. ASME Journal of Mechanism, Transmissions and Automation in Design*, 111: 25-28, 1989.
10. Merlet, J. P., Singularity configurations of parallel manipulators and Grassman geometry, *Int. Journal of Robotics Research*, 8(5): 45-56, 1989.
11. Nguyen, C. C., Antrazi, S. S and Zhen Lie Zhou., Analysis and Implementation of six degrees of freedom Stewart Platform based force sensor for passive compliant robotic assembly, In: *Proc. of IEEE Southeast Conf.*, 880-884, 1991.
12. *NISA II/DISPLAY III Users Manual*, Engineering Mechanics Research Corporation, USA, Version 7, 1997.
13. Paros, J. M. and Weisbord, L., How to design flexure hinges, *Machine Design*, 151-156, 1965.
14. Rees Jones, J., Cross coordinate control of Robot Manipulators, In: *Proc. of the Int. Workshop on Nuclear Robotic Technologies*, 1987.
15. Romiti, A. and Sorli, M., Force and moment measurement system on a robotic assembly hand, *Sensors and Actuators A*, 32: 531-538, 1992.
16. Sorli, M. and Zhmud, N., Investigation of force and moment measurement system for a robotic assembly hand, *Sensors and Actuators A*, 37-38: 651-657, 1993.
17. Stewart, D., A platform with six degrees of freedom, *Proc. of Institution of Mechanical Engineers*, Part 1, 180(15): 371-386, 1965.